




The Effect of Ni and Bi Additions on the Solderability of Sn-0.7Cu Solder Coatings

M.I.I. RAMLI,¹ M.A.A. MOHD SALLEH ^{1,6} M.M.A. ABDULLAH,¹
P. NARAYANAN,² J. CHAIPRAPA,³ R. MOHD SAID,¹ S. YORIYA,⁴
and K. NOGITA⁵

1.—Center of Excellence Geopolymer and Green Technology (CeGeoGTech), School of Materials Engineering, Universiti Malaysia Perlis (UniMAP), Taman Muhibbah, 02600 Jejawi, Arau, Perlis, Malaysia. 2.—Nihon Superior (M) Sdn Bhd, Lot 17, Jalan Industri 1, Free Industrial Zone Jelapang 2, 30020 Ipoh, Perak, Malaysia. 3.—Synchrotron Light Research Institute, Muang District, Nakhon Ratchasima 30000, Thailand. 4.—National Metal and Materials Technology Center, National Science and Technology Development Agency, 114 MTEC, Thailand Science Park, Pahonyothin Road, Khlong Neung, Khlong Luang, Pathum Thani 12120, Thailand. 5.—Nihon Superior Centre for the Manufacture of Electronic Materials (NS CMEM), School of Mechanical and Mining Engineering, The University of Queensland, Brisbane, QLD 4072, Australia. 6.—e-mail: arifanuar@unimap.edu.my

The present investigation explores the influence of Ni and Bi on the solderability of Sn-0.7Cu solder coatings. The minor addition of 0.05 wt.% Ni into the Sn-0.7Cu solder alloy results in an improvement in the wettability based on dipping tests. The solderability investigation using a globule mode shows the influence of Ni and Bi on the interfacial intermetallic compound (IMC). The addition of Ni to a Sn-0.7Cu solder coating resulted in a $(\text{Cu},\text{Ni})_6\text{Sn}_5$ interfacial IMC, which enhanced the solderability performance during the globule test. With an increasing amount of Bi in the Sn-0.7Cu-0.05Ni-xBi solder ball, the surface energy of the solder alloy can be reduced, and this improves the solderability. The synchrotron micro-XRF results indicate that Ni is found in a relatively high concentration in the interfacial layer. Additionally, Bi was found to be homogeneously distributed in the bulk solder, which improved solderability.

Key words: Solderability, intermetallic compound, free solder, solder coating, soldering

INTRODUCTION

The application of surface mount technology (SMT) to position surface mount devices (SMD) on printed circuit boards (PCB) has rapidly grown within the electronics industry.¹ The main advantage of SMT is that it can be mounted onto a PCB without the need for drilled holes on the PCB, which reduces the lower initial manufacturing costs. However, it should be pointed out that the PCB needs to be exposed to a copper-coated surface finish in order

to protect its surface from impurities such as oil, dust, and oxide layers. The surface finish serves two essential purposes: to be solderable and to act as a barrier to prevent oxidation, which, if the latter occurs, could result in subsequent assembly problems. The application of chip scales packages (CSPs) in harsh environments requires a conformal surface finish for meeting reliability requirements. Subsequently, some in the PCB industry believe that PCBs must be coated in order to protect the copper. Given that there is no alternative to solder, PCBs must be soldered using solder as a coating. Functional as a thin coating, the solder can be applied either by dipping or passing the circuit boards over molten solder(s). The solder coating is

(Received May 6, 2019; accepted August 27, 2019; published online September 11, 2019)

designed to improve aesthetics and extend the life of the electronic components. Properties required for solder coating include a low rate of copper dissolution and stable interfacial intermetallic compounds.

A hot air solder levelling (HASL) surface finish is one of the most common surface finishes used in PCBs for substrate manufacturing. HASL utilises solder as a thin coating, which increases its shelf life at lower costs relative to other PCB finishes, such as electroless nickel immersion gold (ENIG), immersion tin (ImSn), and immersion silver (ImAg).² Currently, the application of a solder coating is a highly developed approach. For example, the Sn-Cu-Ni-Ge (SN100CL) solder alloy is one of the most commonly used solder alloys.³ The solderability of solder coating is crucial in the soldering process, as it ensures excellent bonding is formed between the solder material and substrate. If the solder coating is insufficient to provide a layer of free solder, the solderability will decrease due to thinner free solder thicknesses. Therefore, it is crucial to understand how free solder influence the solderability, which is closely related to the wetting force and surface tension. A wetting balance is typically used to evaluate solderability by immersing a substrate in molten solder, and its corresponding wetting force is continually measured as a function of time.⁴ Figure 1a illustrates a typical wetting force curve. Solderability is normally evaluated based on two criteria, namely the wetting time (s) and the maximum force (mN)⁵ as described in Fig. 1b. Although Sn-0.7Cu has been attractive for soldering due to its excellent physical and mechanical characteristic,⁶ its wetting properties are slightly dissatisfactory for solder coating applications⁷ and for process packaging at high densities.⁸ It is also well known that the addition of Ni in Sn-0.7Cu solder improves its wettability properties.⁹ Wang et al.¹⁰ reported that the addition of 0.1% Ni in Sn-2.5Ag-0.7Cu-0.1RE solder alloy increases wettability. In the solder coating, the formation of the interfacial intermetallic compound (IMC) between the solder

and Cu-substrate interface is an indication of chemical bonding. The IMC is immediately formed as the solder melts on the Cu pads and continues to grow when exposed to high temperature. The thick IMC layer formed could also cause a detrimental effect on strength due to the brittle behaviour of the IMC layer.

The properties and mechanical reliability of solder joints are significantly dictated by the condition of solder material, IMC thicknesses and the morphologies of IMC. The interface of the IMC layer is critical towards the mechanical reliability of subsequent electronic devices. Therefore, the growth of the IMC layer during isothermal ageing has been investigated in numerous studies.¹¹ Many studies concluded that IMC thickness increases in tandem with the ageing time. Studies on the IMC layer thickness formation have also revealed the significance of wetting behaviour and interfacial reactions.¹² In our previous study,⁵ we found that higher free solder thickness improves the solderability, where the free solder thickness can be tailored by annealing. We also confirmed that the solderability of Sn-0.7Cu-0.05Ni solder coating improved due to the addition of 60 ppm Ge.

In this study, the effect of the addition of Ni and Bi to the solderability of Sn-0.7Cu solder coating was investigated. This includes understanding the wettability of solders on Cu substrates using the wetting balance test by dipping and the solderability of annealed solder coating with Sn-0.7Cu-0.05Ni-xBi solder alloy using the globule mode method. The results were verified by the wetting time and maximum force for both solder coatings. Following the globule mode test, the distribution of the Bi and Ni element in Sn-0.7Cu and Sn-0.7Cu-0.05Ni was also determined using a synchrotron micro-XRF.

EXPERIMENTAL PROCEDURE

Solder alloy samples were prepared from pure metals in the form of ingots supplied by Nihon Superior Co. Ltd., Japan. Two solders were

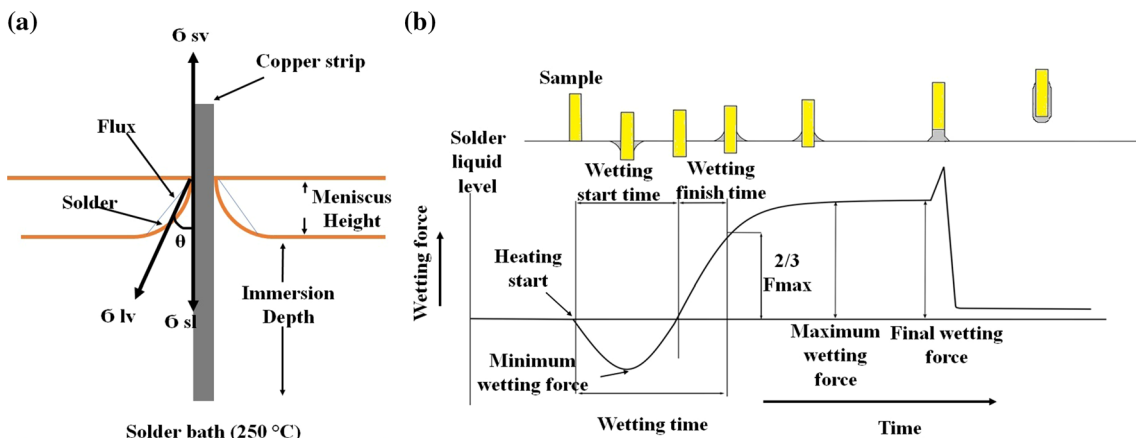


Fig. 1. Schematic diagrams showing the (a) wetting angle measurement and (b) wetting curve by the wetting balance method.

prepared in the form of solder coating consisting of Sn-0.7Cu and Sn-0.7Cu-0.05Ni solder alloy. Solder alloys with different compositions were prepared in an electric resistance furnace at 350°C: Sn-0.7Cu-0.05Ni + 0.5Bi, Sn-0.7Cu-0.05Ni + 1.0Bi, Sn-0.7Cu-0.05Ni + 1.5Bi and Sn-0.7Cu-0.05Ni + 2.0Bi. After 1 h in the furnace, the solder was cast onto a stainless-steel mould and rolled into foils with a thickness of 30 μm . Next, a thin sheet of solder was punched into a diameter of 2.0 mm, then dipped in rosin mildly activated (RMA) flux, and placed on a Pyrex sheet. The sheet solder was then melted in a reflow oven to form a solder ball (spheres) via surface tension.

The wetting balance test was conducted using a Multicore Universal Solderability Tester (MUST) from Gen3 Systems. The copper strip, with dimensions of 3 cm \times 10 cm \times 0.3 cm, was cleaned using an acid cleaning liquid containing 5 g of hydrochloric acid (35%) with 95 g of deionised water (1.75%) to remove surface oxides and contaminants. Prior to the tests, each copper strip was initially dipped in a flux for 2 s, then the flux was drained by placing its vertically on a clean filter paper for 2 s. The flux used was a standard B type (JIS Z3198-4), which is a mixture of rosin, 2-propanol, and diethylamine hydrochloride. The copper strip was then dipped with molten solder for 20 s with an immersion and removal speed set to 30 mm/s. Next, the surface of the solder bath was skimmed to remove the dross at a wetting temperature of 265–270°C. For part one, the copper strip was coated with Sn-0.7Cu and Sn-0.7Cu-0.05Ni by the wetting balance test following the JIS Z3198-4 standard.

Table I summarises the condition of the wetting balance test used in this study. The schematic diagram for the solderability testing is illustrated in Fig. 1a and b. The wetting angle was calculated from the height of the meniscus rise of the molten solder and the wetting force determined by the wetting balance apparatus. The equilibrium wetting angle was determined from the interfacial tensions, σ_{sv} , σ_{sl} and σ_{lv} , via the Young–Dupre equation¹³:

$$\sigma_{sv} - \sigma_{sl} = \sigma_{lv} \cos \theta \quad (1)$$

Next, the coated samples were annealed at 180°C for 24 h, 120 h and 240 h, respectively. The samples were properly treated using an acid cleaning liquid

containing 5 g of hydrochloric acid with 95 g of deionised water to remove the oxidation effect following the annealing process. The samples were then cross-sectioned in order to observe the IMC of the solder coating. The interfacial IMC thickness was measured using Image-J software.

In part two, the solderability testing on the coated annealed specimens was conducted using a Gen3 wetting balance in the “microwetting balance” globule mode with Sn-0.7Cu-0.05Ni-xBi solder ball, as shown in Fig. 2a. In this mode, the sample was fluxed and fixed at an angle in the grip of the wetting balance. The globule mode was then raised until it touches the surface of the copper strips, simultaneously, the instrument begins to measure the force on the copper strips as a function of time and maximum force, as per Fig. 2b and c. Table II summarises the parameters of the wetting test in the globule mode.

The samples were then examined using a synchrotron micro-XRF elemental mapping, which was carried out at the BL6b beamline at the Synchrotron Light Research Institute (SLRI) in Thailand. At the BL6b, the white x-ray beam was produced from a bending magnet and the size of the beam was limited by a circular aperture prior to being focussed using a polycapillary lens to obtain a micro-x-ray beam with a beam size of 30 \times 30 μm^2 onto the specimen. Without a monochromator, the energy of the micro-x-ray beam is 2–12 keV. The specimen was placed 90 degrees to the incident x-ray beam and the CCD camera, while the Vortex EM-650 silicon drift detector used to collect the fluorescent x-rays emitting from the samples was placed 45 degrees to the specimen. The specimens were mounted vertically on the sample holder, and the raster scanning of the samples was performed using high precision motorised stages. The experiments were performed at atmospheric conditions, and the exposure time for each point was 10 s. The result was then analysed using the PyMca software.¹⁴

Elemental mapping was performed using micro-XRF by detecting the characteristic x-rays of the element. This technique is commonly used to analyse the distribution of elements after the globule mode test. The samples, post-globule mode testing, were mounted, ground, and polished prior to being placed onto a glass slide.

RESULTS AND DISCUSSION

Wettability of Solder Coating on the Cu Strip Using the Dipping Method

Figure 3 shows the wettability of Sn-0.7Cu and Sn-0.7Cu-0.05Ni solder alloy on the Cu strip in the context of the wetting time and maximum force applied by the dipping test. Better wettability is determined by a lower wetting time and a higher value of maximum force. The result indicates that the Sn-0.7Cu-0.05Ni solder coating has the highest maximum force and lowest wetting time relative to

Table I. Testing parameters for wetting test in dipping mode

Cu specimen size	10 mm \times 3 mm \times 0.3 mm
Atmosphere	Air
Solder pot temperature	265–270°C
Immersion time	20 s
Immersion depth	5 mm
Immersion speed	30 mm/s

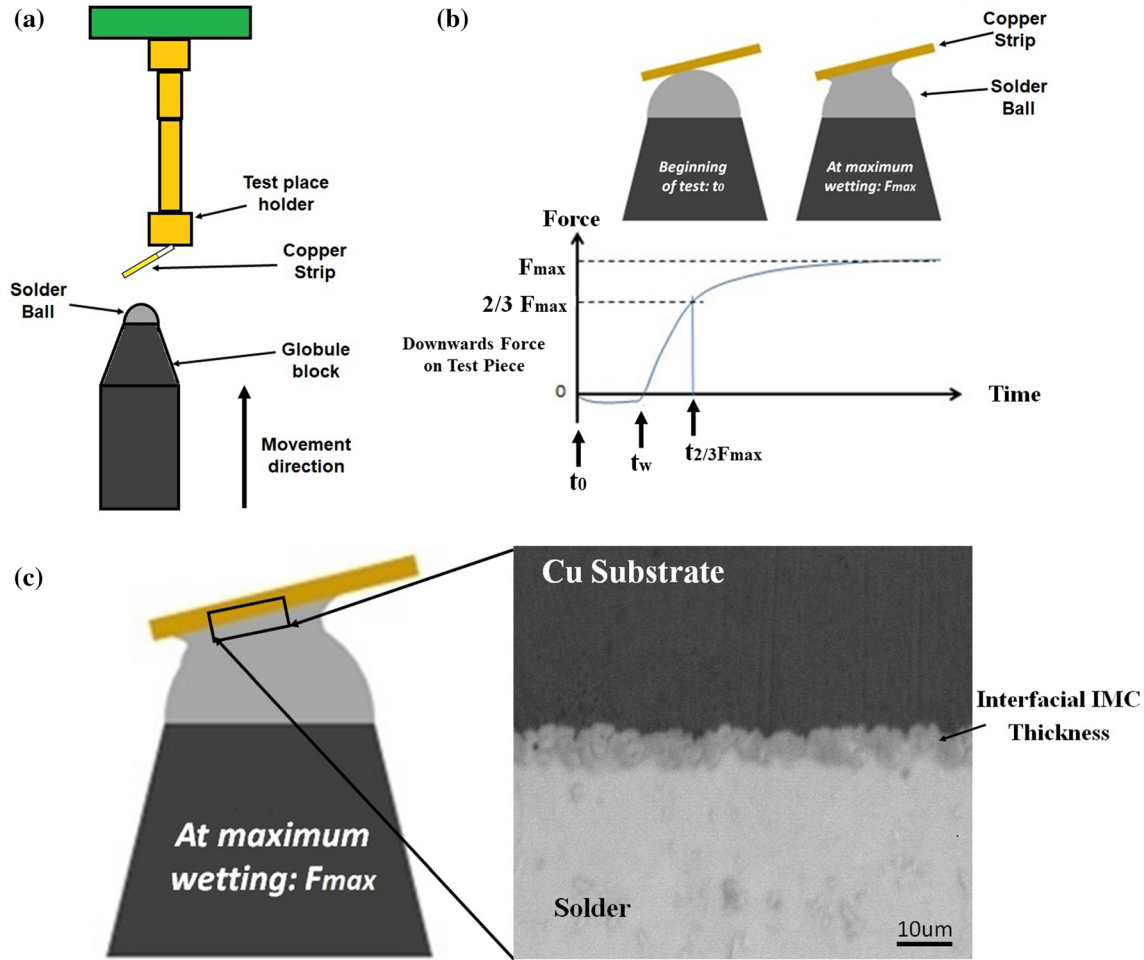


Fig. 2. Wettability test in globule mode schematic diagram (a) side view (b) typical wetting balance curve; t_0 = start point to wet; t_w = peak time, $2/3 F_{max} = 2/3$ from the maximum wetting force, and F_{max} = maximum wetting force and (c) illustration interfacial IMC during the globule mode.

Table II. Testing parameters for the wetting test in globule mode

Parameters	Details
Size of substrate	10 mm \times 3 mm \times 0.3 mm
Substrate material	Copper
Solder ball type	Sn-0.7Cu-0.05Ni-xBi
Globule size	4 mm
Mass of solder	200 mg
Immersion speed	1.0 mm/s
Removal speed	1.0 mm/s
Immersion depth	0.2 mm

that of Sn-0.7Cu solder coating. Accordingly, this confirms that the presence of Ni decreases the surface tension of the molten solder. Wettability is mainly determined by the surface tension between the liquid solder and surrounding flux; the liquid solder quickly accumulates at the solder/flux interface in its molten state.¹⁰

The IMC's thickness is dictated by the diffusion rates of the Cu and Sn via reactions at the layer interfaces. Additionally, IMC and free solder

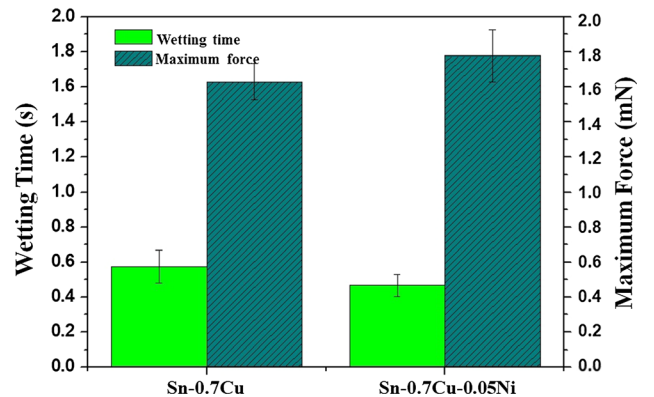


Fig. 3. Relationship between the wetting time and the maximum force.

thicknesses dictate the suitability of solderability when assembling electronic components. However, Sobri et al.¹⁵ hypothesized that increased dipping time increases IMC's thickness, but it should be pointed out that the total coating thickness remains unaffected by differences in the dipping time.

Interfacial Intermetallic Compound (IMC) and the Free Solder Thickness of Sn-0.7Cu and Sn-0.7Cu-0.05Ni Solder Coating Upon Annealing

The coated samples were annealed at multiple times to obtain different interfacial IMC and free solder thicknesses. The cross-sections of the coated

Sn-0.7Cu and Sn-0.7Cu-0.05Ni solder coating after annealing are shown in Fig. 4. In the case of both solder alloys, the Cu_6Sn_5 intermetallic layer in the shape of scallops was formed between the copper strip and solder. Comparing Fig. 4a and b, which show images of the samples prior to the annealing process, the intermetallic layer of the Sn-0.7Cu-

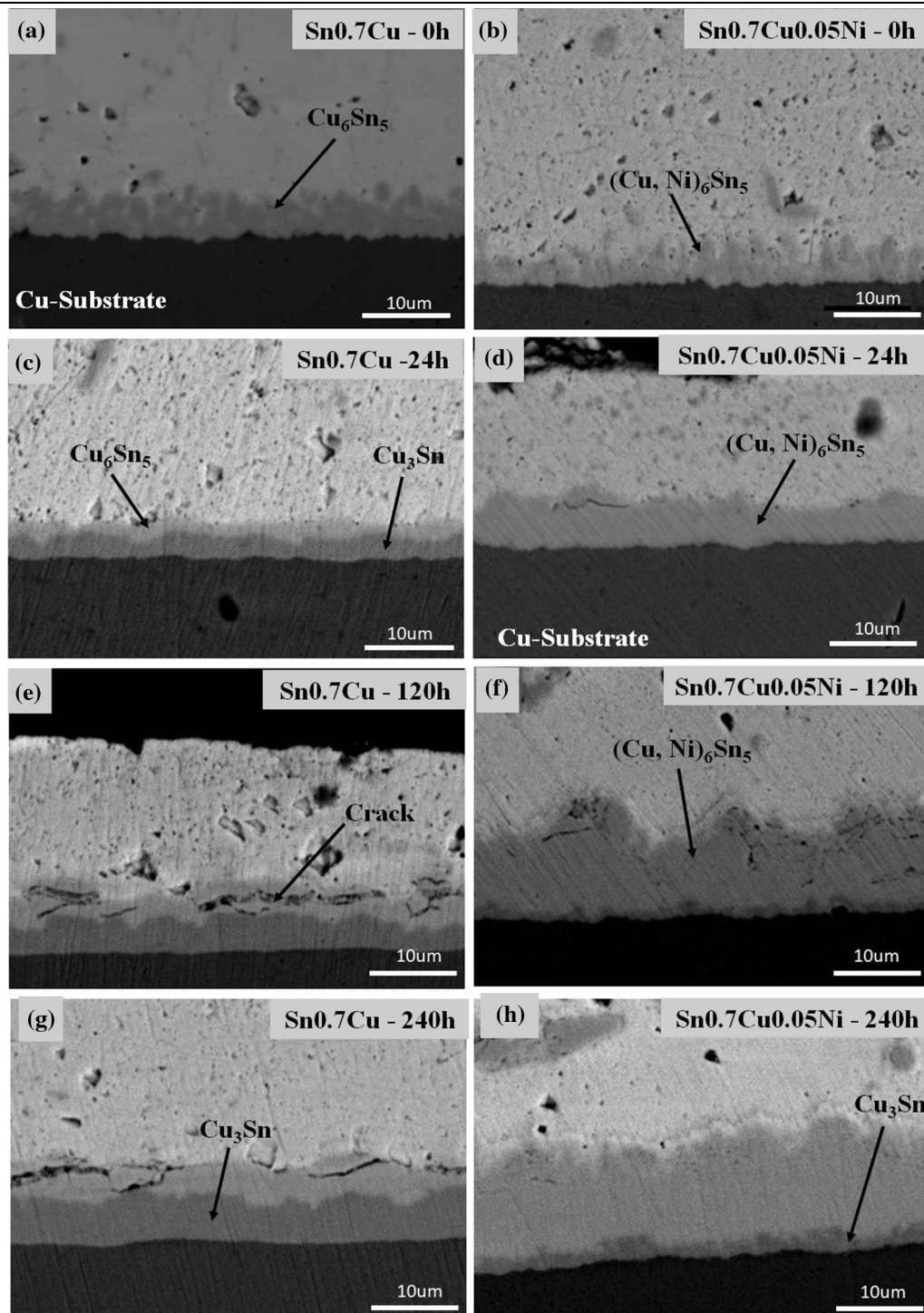


Fig. 4. Growth of IMC in Sn-0.7Cu coating on copper strip as a function of annealing temperature at 180°C for (a) 0 h, (c) 24 h, (e) 120 h and (g) 240 h and Sn-0.7Cu-0.05Ni coating on copper strip as a function of annealing temperature at 180°C for (b) 0 h, (d) 24 h, (f) 120 h and (h) 240 h.

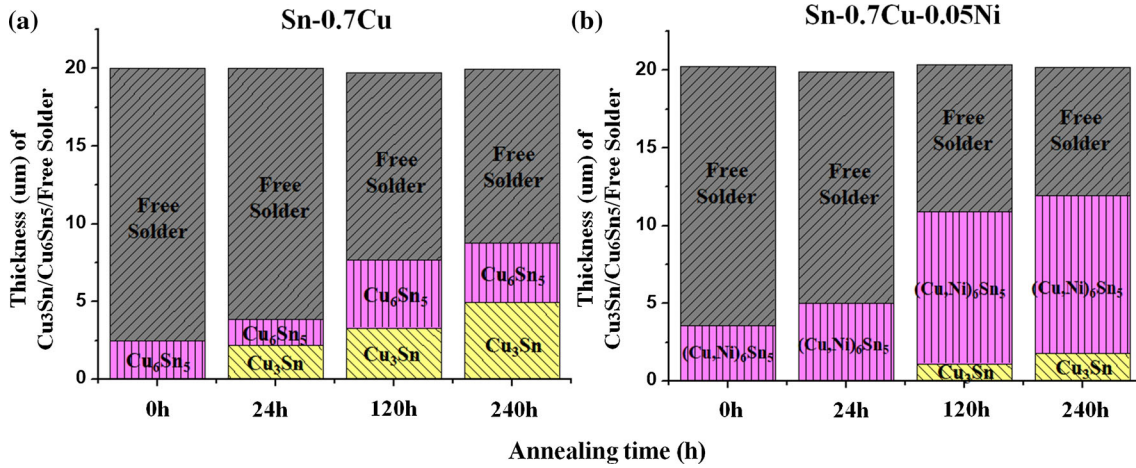


Fig. 5. Average thickness of $\text{Cu}_3\text{Sn}/\text{Cu}_6\text{Sn}_5/(\text{Cu},\text{Ni})_6\text{Sn}_5$ and free solder as a function of annealing time (a) Sn-0.7Cu and (b) Sn-0.7Cu-0.05Ni.

0.05Ni solder was much thinner relative to that of the Sn-0.7Cu solder. For the Sn-0.7Cu solder alloy, after being annealed for 24 h, a layer of Cu_3Sn was formed between the Cu_6Sn_5 layer and the Cu substrate. Also, the scallop-shaped Cu_6Sn_5 layer changed into a planar configuration when annealed. Further annealing at 120 h and 240 h resulted in the Cu_6Sn_5 and Cu_3Sn intermetallic layer thicknesses increasing in tandem with annealing time.

The analyses of the IMC layer's growth and free solder thickness post-annealing was conducted by measuring the average thickness of the total interfacial layer ($\text{Cu}_6\text{Sn}_5 + \text{Cu}_3\text{Sn}$), as per Fig. 5. Generally, increasing annealing time results in thicker interfacial intermetallic layer.¹⁶ The interfacial IMC of the Sn-0.7Cu increased from $3.54 \mu\text{m}$ to $3.85 \mu\text{m}$, $7.70 \mu\text{m}$, and $8.78 \mu\text{m}$ following 24 h, 120 h, and 240 h, respectively. The Cu_3Sn interfacial layer also increased after being annealed for 24 h to $2.18 \mu\text{m}$, and $3.32 \mu\text{m}$ and $4.95 \mu\text{m}$ after 120 h and 240 h of being annealed, respectively. A thin as-reflowed interfacial IMC thickness was detected in the Sn-0.7Cu-0.05Ni measuring $2.45 \mu\text{m}$, which increased to $5.02 \mu\text{m}$, $10.9 \mu\text{m}$, and $13.3 \mu\text{m}$ when annealed for 24 h, 120 h, and 240 h, respectively. The Cu_3Sn interfacial can only be observed after being annealed for 120 h, measuring $1.1 \mu\text{m}$, which increased to $1.79 \mu\text{m}$ after being annealed for 240 h.

With thicker IMCs, the free solder's thickness becomes thinner with increasing annealing times. In the case of the Sn-0.7Cu solder coating, the free solder's thickness decreased from $17.55 \mu\text{m}$ to $17.15 \mu\text{m}$, $12.0 \mu\text{m}$, and $11.2 \mu\text{m}$ after annealing for 24 h, 120 h, and 240 h, respectively. However, in the case of the Sn-0.7Cu-0.05Ni solder coating, the free solder thickness decreased from $16.46 \mu\text{m}$ to $14.90 \mu\text{m}$, $9.1 \mu\text{m}$, and $8.06 \mu\text{m}$ after annealing for 24 h, 120 h, and 240 h, which confirms that the IMC for the Sn-0.7Cu-0.05Ni is much thicker relative to the Sn-0.7Cu solder alloys. It is believed that the solubility of Cu into the molten Sn phase is very low

and the addition of Ni into the molten Sn, increases this solubility with the higher solubility, the dissolution rate increases along with the IMC growth.

Figure 4c, d, e, f and h show the variation of the microstructure of the IMC layer (comparing Cu_6Sn_5 and Cu_3Sn). Post-annealing, cracks on the Sn-0.7Cu coating was evident relative to the Sn-0.7Cu-0.05Ni solder caused by stress generated by the volume change associated with the polymorphic transformation between the η (hexagonal) and η' (monoclinic) transformation that occurred at $\sim 186^\circ\text{C}$, as per Nogita.¹⁷ However, it can be seen that the addition of Ni into Sn-0.7Cu, can stabilise the Cu_6Sn_5 interfacial IMC giving less cracking and suppress the Cu_3Sn interfacial IMC compared to those without the addition of Ni. The addition of Ni will affect the diffusional coefficients and the activation energy of Cu_6Sn_5 . As a phase with a higher interdiffusion coefficient, the IMC will grow with more ease through a solidifying melt. Huang et al.¹⁸ also reported that the activation energy of Cu_6Sn_5 decreases with addition of Ni. This implies that the Ni induces easier nucleation of $(\text{Cu},\text{Ni})_6\text{Sn}_5$, and nucleates preferentially to Cu_3Sn and suppresses its growth.¹⁹ By increasing the diffusion coefficient of Sn in Cu_6Sn_5 , the diffusional driving force of Cu_3Sn is decreased. This give explanations to the suppression of Cu_3Sn with Ni addition.

In the case of Sn-0.7Cu solder coating, at shorter ageing times, the Cu_6Sn_5 layer thickness is thicker relative to the thickness of the Cu_3Sn layer. However, increased ageing time results in the Cu_3Sn layer thickness being almost as thick as the Cu_6Sn_5 layer thickness, as shown in Fig. 4c, e and g. In the Sn-0.7Cu-0.05Ni solder coating, Cu_3Sn is only present when the ageing time is extended, but the thickness remains lower relative to that of the Cu_6Sn_5 layer, as can be seen in Fig. 4f and h. According to Mohd Salleh et al.²⁰ Cu_6Sn_5 would quickly form during the early stage of Sn-0.7Cu solder wetting, with a Cu_3Sn intermetallic layer forming due to continuous Cu diffusion from the Cu

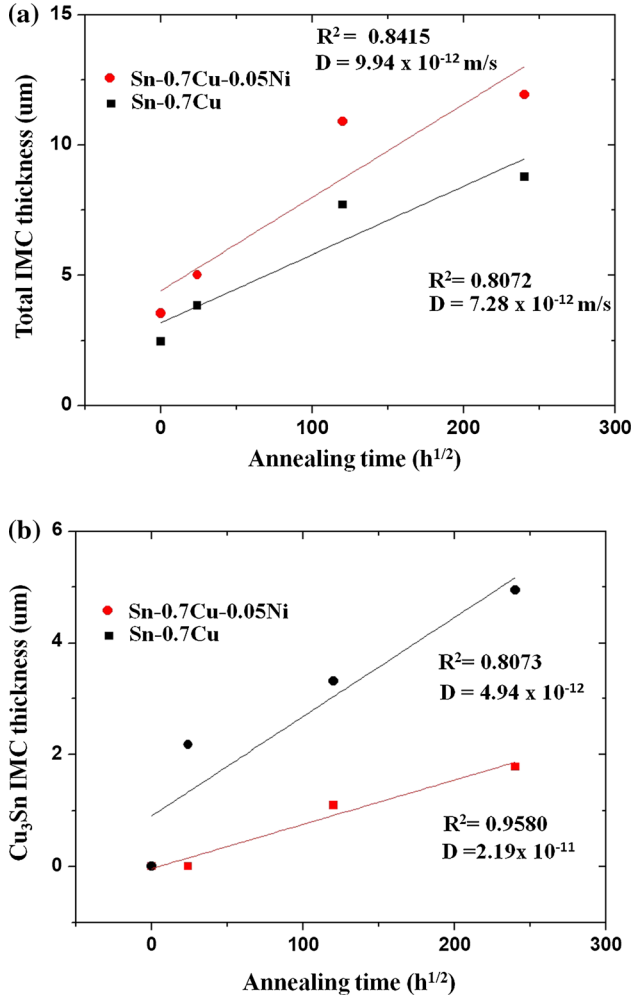


Fig. 6. Growth kinetics of (a) total IMC thickness as a function of annealing time and (b) Cu₃Sn IMC thickness as a function of annealing time.

substrate into the Cu₆Sn₅ layer, which was also supported by Wang et al.²¹ concluded that annealing accelerates the formation of the Cu₃Sn intermetallic layer. In this study, the Cu₃Sn layer in Sn-0.7Cu-0.05Ni was thinner relative to the Cu₃Sn layer in the Sn-0.7Cu, confirming that the addition of Ni suppresses Cu diffusion from the Cu strip into the Cu₆Sn₅ layer.

Figure 6 shows the growth kinetics of IMC as a function of annealing time. The result reveals that the relationship between the thickness of the overall IMC layer and the annealing time adhere to follow Fick's law.

$$y = \sqrt{Dt} \quad (2)$$

Where y is the average IMC thickness, t is the annealing time, and D is the growth rate that is a function of temperature. The growth rate can be determined using a linear regression analysis of y versus \sqrt{t} , where the slope of the straight line is \sqrt{D} .

The growth rate was estimated to elucidate the effect of Ni on the total IMC. As can be seen in Fig. 6a, the growth rate of the addition of Ni for the total IMC is higher relative to the Sn-0.7Cu total of IMC. In the case of the Cu₃Sn growth rate (Fig. 6b), the result confirms that the growth rate for Cu₃Sn is higher without the addition of Ni.

Solderability of Annealed Solder Coating with Sn-0.7Cu-0.05Ni-xBi Solder Alloy

The annealed solder coating was then tested with the Sn-0.7Cu-0.05Ni-xBi solder ball to determine its solderability performance using globule testing. Figure 7a and b shows the wetting time and maximum force of the Sn-0.7Cu solder coating when it touches the Sn-0.7Cu-0.05Ni + xBi solder ball at multiple annealing times. Figure 7c and d also shows the influence of Ni on the Sn-0.7Cu solder coating's solderability with the Sn-0.7Cu-0.05Ni + xBi solder ball. The addition of Ni into the Sn-0.7Cu solder coating resulted in a slight increase in the maximum force and decreased wetting time. Next, the standard (0 h) and more extended (240 h) annealing times were used to elucidate the effect of annealing on solderability. The results showed that when annealed at 240 h, the wetting time of both solder coatings increased and decreased the maximum force(s). Therefore, it is concluded that shorter wetting time and higher maximum force represents excellent solderability.²² Noh et al.²³ reported that increasing maximum force and shorter wetting time would result in superior wettability of solder alloys. As a result of this, the Sn-0.7Cu-0.05Ni solder coating would provide superior solderability relative to the Sn-0.7Cu solder coating.

The observation outlined above can be attributed to the annealing process, which decreases the free solder's thickness, as per Ramli et al.⁵ who suggested that if the interfacial IMC increases, the free solder thickness decreases, which decreases the solderability of the solder's coating. Moreover, the solderability of the solder's coating is engulfed by thicker intermetallic layers and thinner free solder thicknesses. In this example, the IMC growth of the solder coating increases in tandem with increasing annealing time, which can be attributed to the dissolution of Cu substrate to the solder and interdiffusion kinetics from thermal acceleration caused by annealing.²⁴ However, it should be pointed out that thicker IMCs produces thinner free solder thicknesses. Generally, thicker free solders provide a higher wettable surface for the soldering process, which engulf the interfacial IMC thickness, thus improving wettability performance.

The relationship between the free solder thickness and solderability of the annealed coated samples was determined using the wetting time and the maximum force reported by the experiment. Here, the wetting time represents the wetting rate and

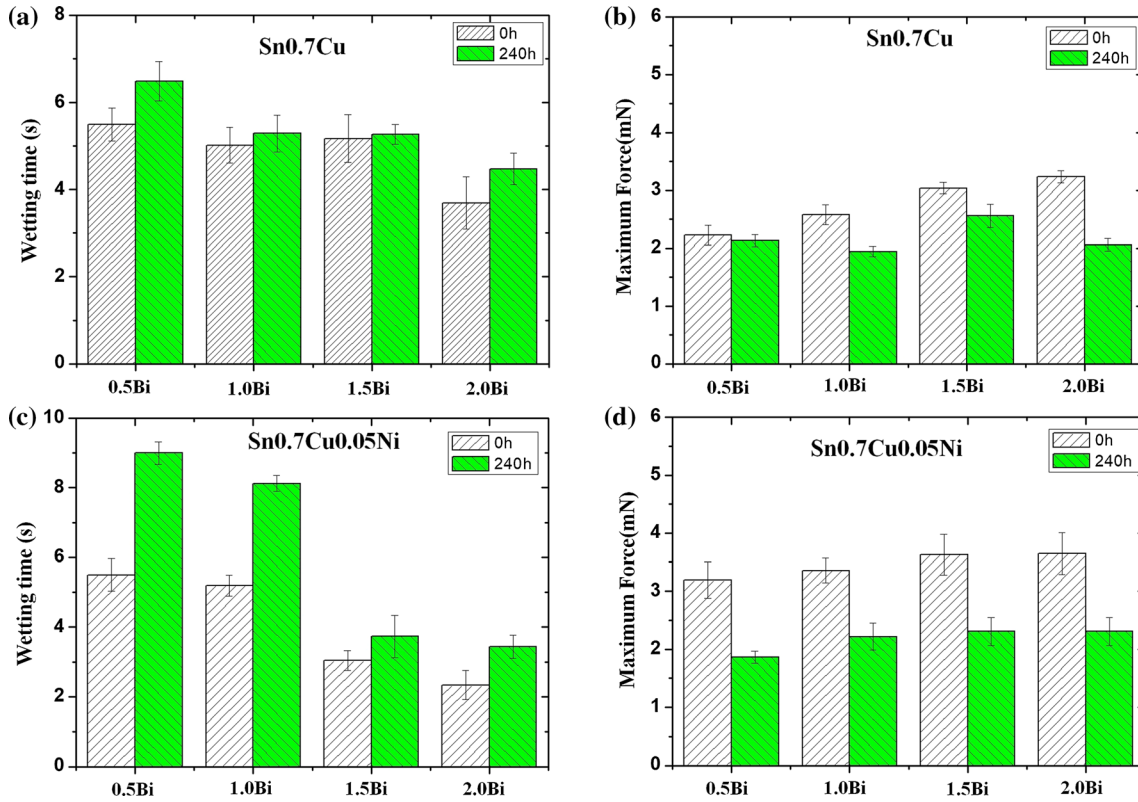


Fig. 7. Effect of Sn-0.7Cu-0.05Ni-xBi solder ball on wetting time, (a) Sn-0.7Cu coating, (c) Sn-0.7Cu-0.05Ni coating and on maximum force, (b) Sn-0.7Cu coating and (d) Sn-0.7Cu-0.05Ni coating.

simulates the actual conditions in soldering applications. The wetting time was taken at $2/3 F_{max}$, which was used to determine the kinetics of soldering. In addition to the wetting time, the maximum force also showed a significant difference in determining the solderability of the solder. In this case, the annealed sample will influence the coating surface by creating an oxide layer on the surface, which increase the IMC layer's thickness.²⁵ Similarly, the presence of an oxide layer can influence the wetting behaviour, due to its incorporating contaminants from its surroundings. However, this oxide layer can be removed using acid cleaning and flux prior to the globule mode test.²⁶

Next, the Bi element was added to the Sn-0.7Cu-0.05Ni solder ball, which enhanced the solderability of the Sn-0.7Cu and Sn-0.7Cu-0.05Ni solder coating by decreasing the wetting time and increasing the maximum force of the solder ball. This phenomenon can be attributed to the decrease in the surface tension of molten solder by Bi. Nobari et al.²⁷ outlined the effect of the addition of Bi to the Sn-Cu and Sn-Ag-Cu alloys improving wetting and spreading performance. It has also been shown that increasing the amount of Bi decreases the wetting time continuously while increasing the maximum force. Among the solder ball compositions used in this study, the Sn-0.7Cu-0.05Ni + 2.0 Bi solder ball reported the best wetting behaviour in the context

of wetting time and maximum force, as illustrated in Fig. 7.

Figure 8 shows the microstructure of the cross-sectioned samples following the globule mode being used on the wetting balance tests. During the dipping process, the solder reacts with the Cu strip to form a continuous Cu_6Sn_5 IMC at the Cu strip (as shown in the yellow line). This initial formation of the Cu_6Sn_5 IMC at the interface between the solder and Cu-substrate was rapid and almost instantaneous.²⁸ Post-annealing, the intermetallic Cu_6Sn_5 grows, resulting in the formation of very thin Cu_3Sn . With increasing annealing time(s), the IMC's thickness will both increase and decrease the free solder's thickness. The relationship between the IMC thickness and free solder thickness with the wetting time and maximum force has been studied previously.⁵ In the case of the Sn-0.7Cu solder coating, it was confirmed that when the free solder thickness decreased, the wetting time slightly increased. However, despite the fact that the free solder thickness decreases with annealing time, the addition of Bi on Sn-0.7Cu-0.05Ni solder ball decreased the wetting time.

In the case of the Sn-0.7Cu-0.05Ni solder coating (Fig. 8d, e and f), it was found that the IMC's thickness increased and the free solder's thickness decreased post-annealing. The solderability of the solder coating got significantly worse if the free

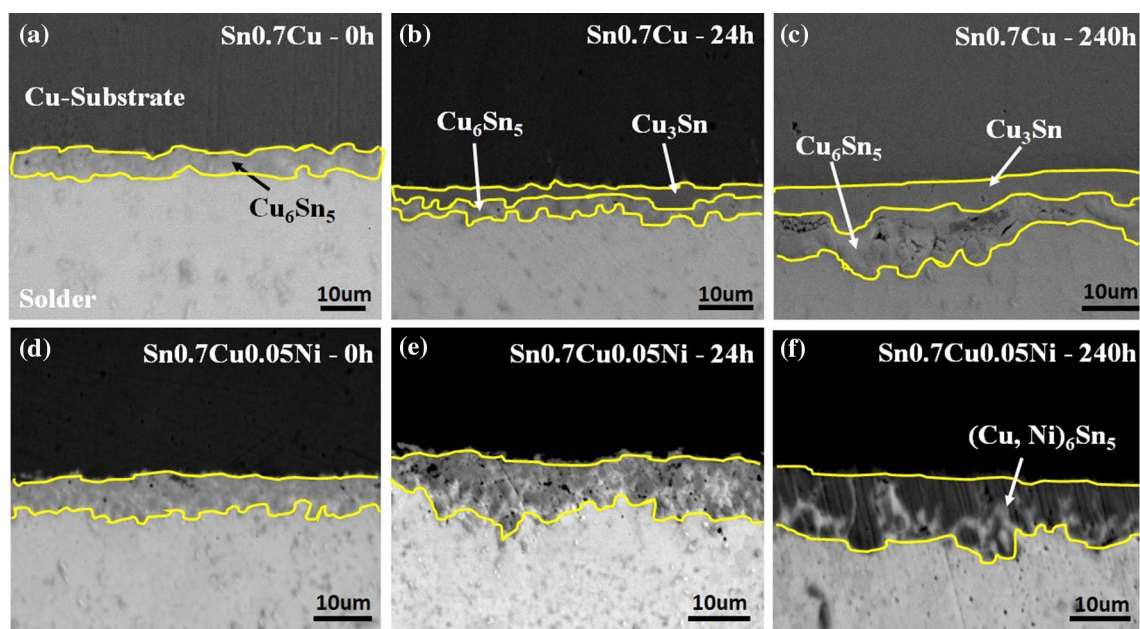


Fig. 8. Micrographs of cross-sectional interfacial IMC after the globule mode test with the Sn-0.7Cu-0.05Ni-2.0Bi solder ball. Sn-0.7Cu solder coating annealing at (a) 0 h, (b) 24 h, (c) 240 h and Sn-0.7Cu-0.05Ni solder coating at (d) 0 h, (e) 24 h, (f) 240 h.

solder thickness decreases. Despite the fact that it was touched by the Sn-0.7Cu-0.05Ni + 2.0Bi solder ball during the globule mode testing, it still results in the best solderability at a lower wetting time and higher maximum force. This observation suggests that the addition of Bi influence the solderability of the solder coating. Furthermore, by comparing both solder coatings, the Sn-0.7Cu-0.05Ni solder coating gives better solderability relative to the Sn-0.7Cu solder coating when tested using the globule mode method with the Sn-0.7Cu-0.05Ni + 2.0Bi solder ball. This finding can be used to determine the influence of the Ni element, which influences the solderability of the solder coating. In the Sn-0.7Cu-0.05Ni solder coating, the intermetallic layer interface corresponds to $(\text{Cu,Ni})_6\text{Sn}_5$ relative to the Cu_6Sn_5 in Sn-0.7Cu solder coating. This observation may be an essential factor that influences the solderability of the solder coating. Furthermore, it also appears that the Bi element did not precipitate in the interfacial IMC layer, which means that it possibly dissolved in the Sn due to the solid-solution mechanism. This occurrence could potentially improve solderability.

Because the addition of Bi remained unreactive with the interfacial IMC layer, further characterization was employed to elucidate the effects of Ni and Bi in Sn-0.7Cu-0.05Ni to its overall solderability. The synchrotron micro-XRF mapping was used to analyse the composition and distribution of the elements in the Sn-0.7Cu and Sn-0.7Cu-0.05Ni solder coating after using the globule mode with

the Sn-0.7Cu-0.05Ni-1.5Bi solder ball. The globule mode was carried out in the y-axis direction so that the Cu-substrate was located at the top and the solder was at the bottom. Figure 9 shows the results of micro-XRF in Sn-0.7Cu and Sn-0.7Cu-0.05Ni solder coatings. The elemental map of the Sn, Cu, Ni and Bi at the solder coating after the globule mode shows the distribution of the elements. The higher intensity indicates a higher concentration of a particular element.

After using the globule mode method with the Sn-0.7Cu-0.05Ni-1.5Bi solder ball, the Cu and Ni elements were distributed throughout the Sn-grain in the bulk solder, which likely formed as $(\text{Cu,Ni})_6\text{Sn}_5$ primary IMC in Sn-0.7Cu coating, as shown in Fig. 9a. Figure 9b shows that when soldered with the Sn-0.7Cu-0.05Ni solder coating, the Ni was not only distributed in the bulk solder as $(\text{Cu,Ni})_6\text{Sn}_5$ primary IMC, but it was also present in the interfacial IMC as $(\text{Cu,Ni})_6\text{Sn}_5$. This observation confirms that the Sn-0.7Cu solder coating formed a Cu_6Sn_5 interfacial IMC and that the Sn-0.7Cu-0.05Ni solder coating form the $(\text{Cu,Ni})_6\text{Sn}_5$ interfacial IMC.

It was also found that during the globule mode method, Ni in Sn-0.7Cu-0.05Ni-xBi solder ball did not diffuse into the interfacial IMC and form a $(\text{Cu,Ni})_6\text{Sn}_5$ interfacial IMC, as proposed in Fig. 10. This might be due to Ni lacking time to diffuse into the Cu_6Sn_5 interfacial IMC from the rapid globule mode test. It was also confirmed that Ni did not melt and form a new interfacial IMC during the globule

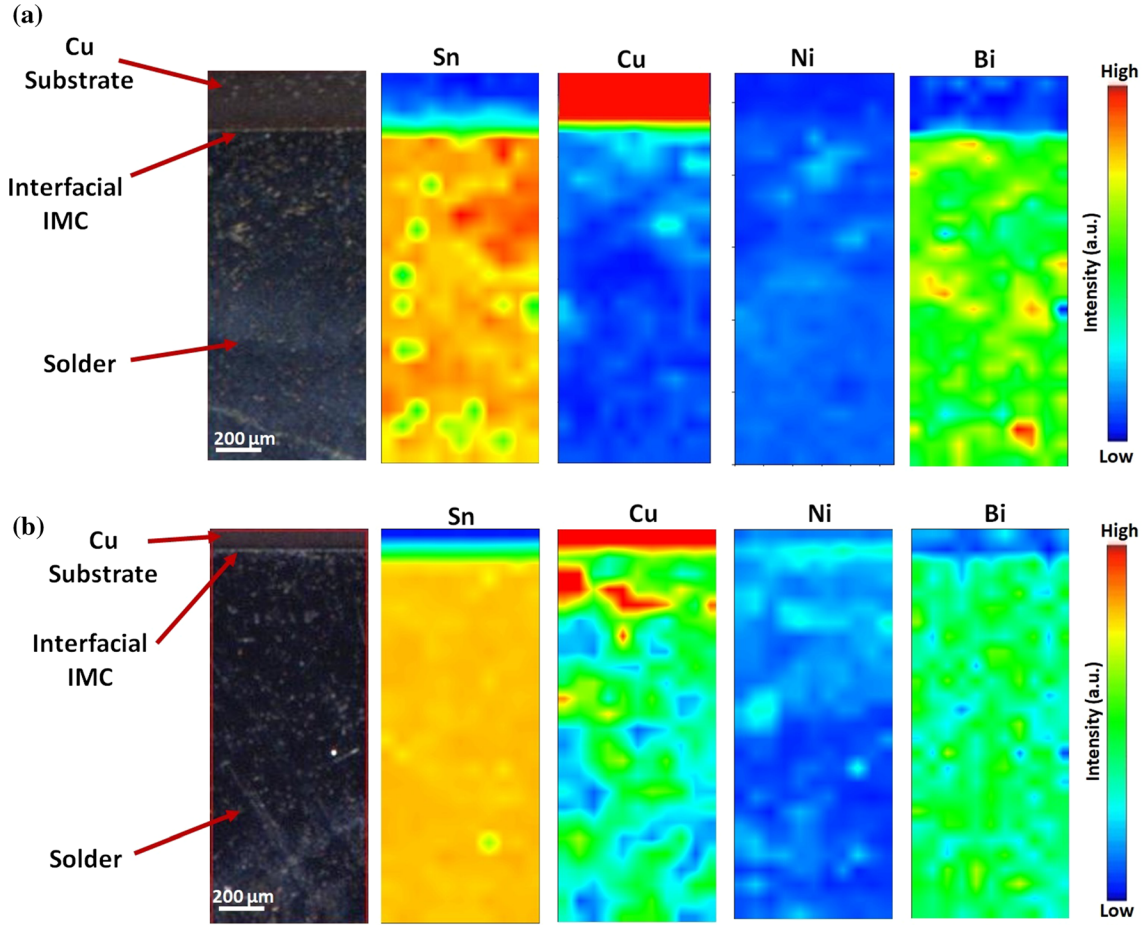


Fig. 9. Micro-XRF mappings after the globule mode test with Sn-0.7Cu-0.05Ni + 1.5Bi solder ball, (a) Sn-0.7Cu coating at 0 h and (b) Sn-0.7Cu-0.05Ni coating at 0 h.

mode test. This is because the IMC of Cu_6Sn_5 was reported to melt at 415°C , and Cu_3Sn IMC at 676°C .²⁹ Owing to this factor, the Cu_6Sn_5 interfacial IMC will not form $(\text{Cu},\text{Ni})_6\text{Sn}_5$ with Ni addition during the globule test. This finding also confirmed the influence of Ni in the interfacial IMC as increasing the solderability of the solder alloy. Wang et al.¹⁰ reported that the addition of Ni up to 0.5 wt.% improved the solderability of the Sn-2.5Ag-0.7Cu-0.1RE solder alloy. The influence of Ni in the interfacial IMC is believed to influence the solderability when using the globule mode test with the Sn-0.7Cu-0.05Ni-xBi solder ball. Furthermore, the addition of Bi in Sn-0.7Cu-0.05Ni solder also increases the solderability of the solder alloy.

The surface energy of the solder is an important criteria in its wetting phenomena. If the surface energy of the copper substrate changes upon the addition of the molten solder, the copper substrate will be wet. This wetting phenomenon can be defined by:

$$S = \gamma_{\text{substrate}} - \gamma_{\text{liquid solder}} - \gamma_{\text{substrate-liquid solder}} \quad (3)$$

where S is the spreading parameter, $\gamma_{\text{substrate}}$ the surface energy of the copper substrate, $\gamma_{\text{liquid solder}}$ the surface energy of the solder, and $\gamma_{\text{substrate-liquid solder}}$ the interfacial energy between the copper substrate and the liquid. If $S < 0$, the liquid solder partially wets the substrate and if $S > 0$, the liquid solder completely wets the substrate. Therefore, if the surface energy of liquid is lower than surface energy of the substrate, more complete wetting will occur. In this study, the author believes that the Bi element in Sn-0.7Cu-0.05Ni-xBi could decrease the surface energy of solder alloy. Indeed, this Bi was found to be well distributed in the β -Sn, which acts as a solid solution strengthening, which decreases the surface tension of solder alloys from the addition of Bi, as per Nobari et al.²⁷ The combination of Ni in the interfacial IMC and Bi makes the solderability

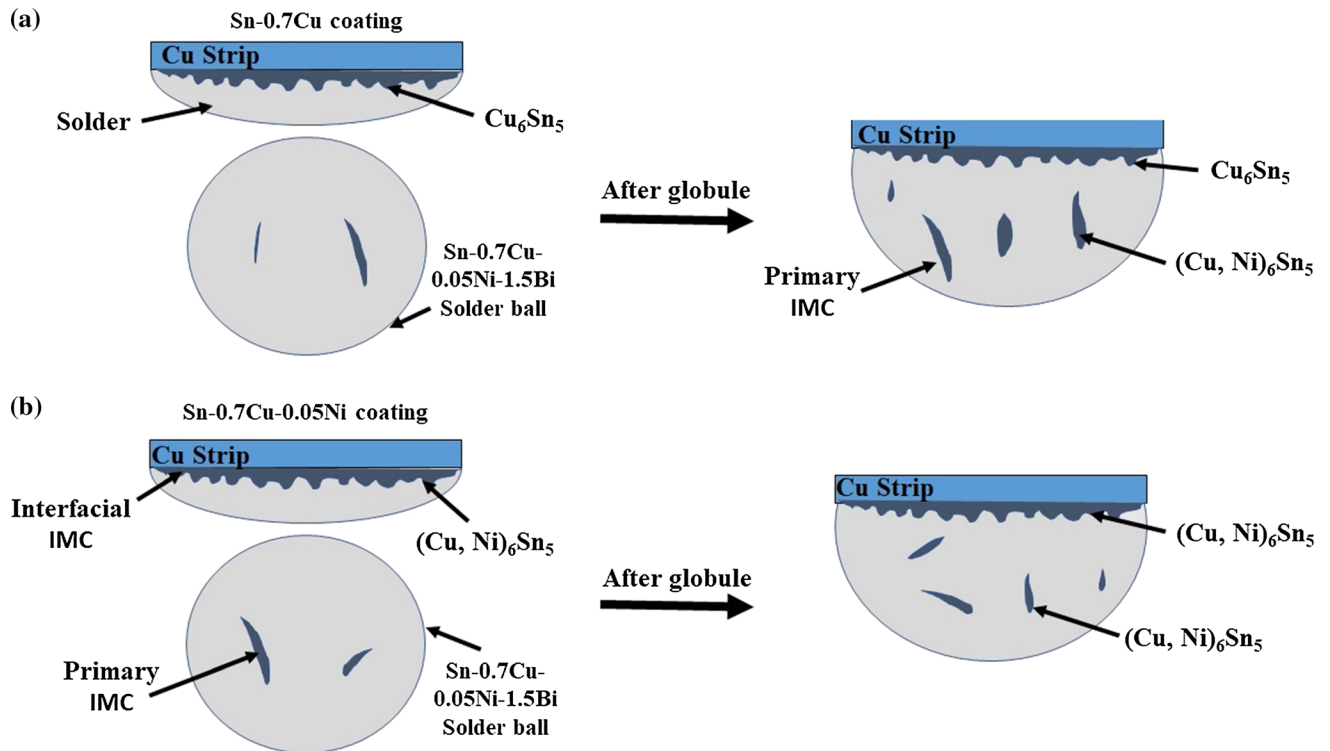


Fig. 10. Proposed mechanisms after the globule mode test with Sn-0.7Cu-0.05Ni-1.5Bi solder ball, (a) Sn-0.7Cu coating at 0 h and (b) Sn-0.7Cu-0.05Ni coating at 0 h.

of Sn-0.7Cu-0.05Ni solder coating superior to the Sn-0.7Cu solder coating.

CONCLUSION

This study elucidated the relationship between solderability and intermetallic thickness of the solder coating. The influence of the combined addition of Ni and Bi to the solderability of solder coating was also established. It can also be concluded that:

1. The Sn-0.7Cu-0.05Ni solder alloy showed better wettability on a Cu substrate relative to the Sn-0.7Cu solder alloy based on the dipping test.
2. The growth kinetics of the total interfacial IMC (Cu_6Sn_5 and Cu_3Sn) of Sn-0.7Cu-0.05Ni solder coating was 9.94×10^{-12} m/s, which is higher relative to the Sn-0.7Cu solder coating, while the growth kinetics of Cu_3Sn in Sn-0.7Cu exceeded that of the Sn-0.7Cu-0.05Ni solder coating.
3. The Ni in Sn-0.7Cu solder coating formed $(\text{Cu}, \text{Ni})_6\text{Sn}_5$ interfacial IMC, while Ni in Sn-0.7Cu-0.05Ni + xBi soldered on Sn-0.7Cu coating did not affect the formation of $(\text{Cu}, \text{Ni})_6\text{Sn}_5$ interfacial IMC, but mostly the primary IMC in the bulk solder.
4. The addition of 2.0 wt.% of Bi in Sn-0.7Cu-0.05Ni solder demonstrated excellent solderability on Sn-0.7Cu-0.05Ni solder coating, with a low wetting time (2.33 s) and a high maximum force (3.65 mN).
5. The addition of Bi in Sn-0.7Cu-0.05Ni improved the surface energy of the solder alloy, which also improves the wetting performance of the solder, where the Bi element was observed to be homogeneously distributed in the β -Sn after soldering.

ACKNOWLEDGMENTS

The authors gratefully acknowledge Nihon Superior (Grant No. 2016/10/0001) and fundamental research grant scheme (FRGS)(FRGS/1/2017/TK05/UNIMAP/02/7) (9003-00635) for the materials and finance support. Wetting balance test were conducted at Nihon Superior (M) Sdn Bhd, Ipoh, Malaysia. The μ -XRF trace element mapping technique was performed at the Synchrotron Light Research Institute (SLRI), Thailand, under Project ID: 3774 and 3774-7.

REFERENCES

1. C.C. Tu and M.E. Natishan, *Solder. Surf. Mt. Technol.* 12, 10–15 (2000).
2. W. Li, in *2015 16th International Conference on Electronic Packaging Technology (ICEPT)*, pp. 538–541 (2015).
3. K. Sweatman, *Global SMT & Packaging*, pp. 10–18 (2009).
4. P. Harant and F. Steiner, in *30th International Spring Seminar on Electronics Technology*, pp. 388–392 (2007).
5. M.I.I. Ramli, M.A.A. Mohd Salleh, F.A. Mohd Sobri, P. Narayanan, K. Sweatman, and K. Nogita, *J. Mater. Sci. Mater. Electron.* 30, 3669–3677 (2019).
6. H. Wang, F. Wang, F. Gao, X. Mac, and Y. Qian, *J. Alloys Compd.* 433, 302–305 (2007).

7. K.N. Prabhu, *World Acad. Sci. Eng. Technol. Int. J. Chem. Mol. Nucl. Mater. Metall. Eng.* 7, 25–28 (2013).
8. G. Zeng, S.D. McDonald, G. Qinfen, Y. Terada, K. Uesugi, H. Yasuda, and K. Nogita, *Acta Mater.* 83, 357–371 (2015).
9. X. Hu, Y. Lai, X. Jiang, and Y. Li, *J. Mater. Sci.: Mater. Electron.* 29, 18840–18851 (2018).
10. Y. Wang, G. Wang, K. Song, and K. Zhang, *Mater. Des.* 119, 219–224 (2017).
11. L. Zhang, S.B. Xue, G. Zeng, L.L. Gao, and H. Ye, *J. Alloys Compd.* 510, 38–45 (2012).
12. J. Liang, N. Dariavach, P. Callahan, and D. Shangguan, *Mater. Trans.* 47, 317–325 (2006).
13. H.Y. Lee, A. Sharma, S.H. Kee, Y.W. Lee, J.T. Moon, and J.P. Jung, *Electron. Mater. Lett.* 10, 997–1004 (2014).
14. V.A. Solé, E. Papillon, M. Cotte, P. Walter, and J. Susini, *Spectrochim. Acta B* 62, 63–68 (2007).
15. F.A. Mohd Sobri, M.A.A. Mohd Salleh, C.M. Ruzaidi, and P. Narayanan, *Appl. Mech. Mater.* 754, 493–497 (2015).
16. M.A.A. Mohd Salleh, S.D. McDonald, and K. Nogita, *J. Mater. Process. Technol.* 242, 235–245 (2017).
17. K. Nogita, *Intermetallics* 18, 145–149 (2010).
18. K.C. Huang, F.S. Shieu, Y.H. Hsiao, and C.Y. Liu, *J. Electron. Mater.* 41, 172–175 (2012).
19. K. Nogita, B. Kefford, J. Read, and S.D. McDonald, *Mater. Sci. Forum* 857, 53–57 (2016).
20. M.A.A. Mohd Salleh, S.D. McDonald, H. Yasuda, A. Sugiyama, and K. Nogita, *Scr. Mater.* 100, 17–20 (2015).
21. K.-K. Wang, D. Gan, and K.-C. Hsieh, *Thin Solid Films* 562, 398–404 (2014).
22. M.J. Rizvi, C. Bailey, Y.C. Chan, and H. Lu, *J. Alloys Compd.* 438, 116–121 (2007).
23. B.I. Noh, J.H. Choi, J.W. Yoon, and S.B. Jung, *J. Alloys Compd.* 499, 154–159 (2010).
24. A.T. Wu, M.H. Chen, and C.N. Siao, *J. Electron. Mater.* 38, 252–256 (2009).
25. P. Yao, P. Liu, and J. Liu, *J. Alloys Compd.* 462, 73–79 (2008).
26. F. Gao, K. Rajathurai, Q. Cui, G. Zhou, I. NkengforAcha, and G. Zhiyong, *Appl. Surf. Sci.* 258, 7507–7514 (2012).
27. A.H. Nobari, M. Maalekian, K. Seelig, and M. Peguleryuz, *J. Electron. Mater.* 46, 4076–4084 (2017).
28. Z.Q. Li, S.A. Belyakov, J.W. Xian, and C.M. Gourlay, *J. Electron. Mater.* 47, 84–95 (2017).
29. T.-T. Luu and A. Duan, Knut E Aasmundtveit and Nils Hoivik, *J. Electron. Mater.* 42, 3582–3592 (2013).

Publisher's Note Springer Nature remains neutral with regard to jurisdictional claims in published maps and institutional affiliations.